Thermodynamic Evidence for Nanoscale Bose-Einstein Condensation in ^{4}He Confined in Nanoporous Media

Keiichi Yamamoto, Yoshiyuki Shibayama, and Keiya Shirahama
Department of Physics, Keio University, Yokohama 223-8522, Japan
(Received 23 November 2007; revised manuscript received 8 January 2008; published 15 May 2008)

We report the measurements of the heat capacity of ^{4}He confined in nanoporous Gelsil glass that has nanopores of 2.5-nm diameter at pressures up to 5.3 MPa. The heat capacity has a broad peak at a temperature much higher than the superfluid transition temperature obtained using the torsional oscillator technique. The peak provides definite thermodynamic evidence for the formation of localized Bose-Einstein condensates on nanometer length scales. The temperature dependence of the heat capacity is described well by the excitations of phonons and rotons, supporting the existence of localized Bose-Einstein condensates.

DOI: 10.1103/PhysRevLett.100.195301 PACS numbers: 67.25.dr, 67.25.de

Bose systems in periodic or random potentials offer a wide variety of novel phenomena and are a topic of great interest in condensed matter physics. In ultracold atoms subjected to a periodic potential, a superfluid-insulator quantum phase transition (QPT) has been reported [1]. The introduction of disorder to an optical lattice induces a state without long range phase coherence, which is considered to be a Bose glass [2]. Superconducting films [3] and Josephson-junction arrays [4] have also been studied as a disordered Bose system.

^{4}He in porous media is one of the ideal systems for studying Bose-Einstein condensation (BEC) in an external potential. By confining ^{4}He in porous media, one can freely control the various experimental parameters such as dimension, topology, and disorder [5–8]. Recently, we have discovered a novel behavior of ^{4}He confined in a porous Gelsil glass by torsional oscillator (TO) studies [9] and pressure measurements (see Fig. 3) [10], where the Gelsil glass is characterized by a three-dimensional (3D) random network of nanopores of 2.5-nm diameter. The TO studies revealed that the superfluid transition temperature T_c is dramatically suppressed by pressurization. At 3.4 MPa, T_c is suppressed to 0 K, which indicates the existence of a QPT at a critical pressure $P_c = 3.4$ MPa. The pressure measurements revealed that the nonsuperfluid (NSF) state, which has very small entropy, exists between the superfluid and solid phase down to 0 K.

The nature of the low-entropy NSF state must be entirely different from the usual normal liquid of bulk ^{4}He. Neutron scattering measurements for ^{4}He in various porous media have shown the existence of BEC even above T_c [11–13]. A theoretical calculation of a strongly correlated Bose fluid in a random potential suggests that there are localized condensates above a critical pressure P_c [14]. These studies imply that the NSF state is a localized state of BEC. However, the entire nature of the state, especially the localized Bose condensation temperature, was not clarified by our pressure measurements. Here we report heat capacities of ^{4}He in Gelsil, and demonstrate a definite evidence for localized BEC on nanometer length scales in the nanopores.

We have employed four Gelsil disk samples which are the same ones as in our pressure studies [10]. These are taken from the same batch as that used in our TO study [9]. Since the sample preparation could affect T_c [9,15,16], the samples were vacuum heat-treated with exactly the same condition as the TO study, which was 423 K, before mounting to the sample cell. The details of the experimental setup were described elsewhere [17].

We measure the heat capacities by the relaxation and the adiabatic heat-pulse method, depending on the external relaxation time of the cell to the thermal bath τ_1 and the thermal relaxation time inside the sample τ_2. In the measurements of the empty cell, τ_1/τ_2 are 6–7 above 0.45 K and we employed the relaxation method [18]. When we introduce ^{4}He into the cell, τ_1/τ_2 usually exceeds 20. This condition is sufficient to employ the adiabatic heat-pulse method. The heat capacity of the empty cell is 3%–31% of that of ^{4}He in the nanopores depending on temperature.

We measure the heat capacities at pressures from 0.25 to 5.27 MPa. At $P < 2.5$ MPa, the pressure is controlled by a room-temperature gas handling system. At $P > 2.5$ MPa, we measured heat capacities along the isochore using the blocked capillary method [10]. After the solidification of bulk ^{4}He in the open space around the Gelsil disks in the sample cell, the ^{4}He samples were annealed by maintaining the cell within 50 mK of the bulk freezing temperature for 10 h to improve the crystallinity of bulk solid in the open space. The pressure is measured *in situ* by a capacitive pressure gauge [10].

In Fig. 1, we show the heat-capacity data at various pressures; here, ^{4}He in the nanopores is in the liquid state. Figure 1(a) show the results at $P < 2.5$ MPa. The heat capacity shows a sharp peak around 2 K and a shoulder around 1.8 K. The sharp peak originates from the λ transition of bulk liquid ^{4}He in the open space. Solid lines

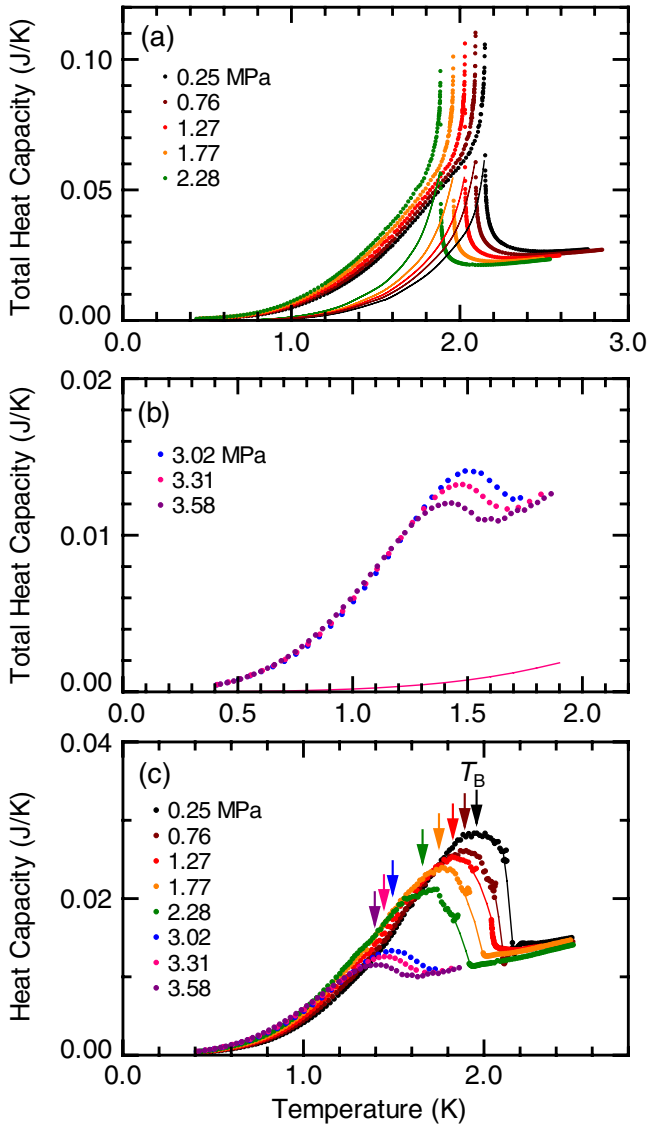

FIG. 1 (color online). Heat capacities at pressures where ^{4}He in the nanopores is in the liquid state. (a) Total heat capacity below 2.5 MPa. The solid lines indicate the heat capacity of bulk ^{4}He in the open volume of the sample cell. (b) Total heat capacity at pressures at $3.02 < P < 3.58$ MPa where bulk ^{4}He solidifies but ^{4}He in the nanopores remains liquid. The solid line is the heat capacity of bulk solid ^{4}He in the open space at 3.31 MPa. (c) The heat capacity after subtracting the contribution of bulk ^{4}He in the open space at $0.25 < P < 3.58$ MPa. The heat capacities show a broad peak at a temperature denoted as T_B. The solid lines are guides to the eye.

indicate the heat capacities of bulk ^{4}He obtained by using the existing specific heat data [19,20]. We estimated the quantity of bulk liquid from these data by the method developed by Zassenhaus and Reppy [21]. The detailed procedure of the estimation was presented elsewhere [17]. The bulk liquid quantity and the density of bulk liquid lead to a nearly constant volume of the open space of 38.5 mm^3, which is comparable to the value of 31 mm^3 estimated from the dimension of the cell and Gelsil disks.

In Fig. 1(b), we show the heat capacity at $3.02 < P < 3.58$ MPa, where ^{4}He in the open space solidifies but ^{4}He in the nanopores remains liquid [10]. The solid line is the heat capacity of bulk solid ^{4}He at 3.31 MPa [22]. We estimated the amount of bulk solid in the open space using the estimated value of 38.5 mm^3 for the open volume and the density of solid ^{4}He. The bulk contribution is much smaller than the "all-liquid" case in Fig. 1(a).

The heat-capacity data of liquid ^{4}He in the nanopores obtained by the subtraction of the bulk contribution are shown in Fig. 1(c). All the data have a clear peak at a temperature denoted as T_B. As pressure increases, both T_B and the peak height decrease monotonically. The heat capacity below 2.5 MPa resembles the data at higher pressures at which the heat capacity of bulk solid ^{4}He is negligibly small. This fact justifies the subtraction of the heat capacity of bulk ^{4}He at $P < 2.5$ MPa.

In Fig. 2, we show the heat capacities at $P > 4.45$ MPa, where ^{4}He in the nanopores is solid [10], with the liquid data at 3.58 MPa. The heat capacity has a peak at a temperature T_M. The peak resembles the peak of liquid at lower pressures. However, in contrast to the case of liquid, T_M and the peak height *increase* with pressure. In the pressure studies [10], the melting onset on heating was observed at $T_{MO} \simeq 1$ K (see Fig. 3). Thus, the heat-capacity peak at T_M is attributed to the latent heat of melting. Contrary to ordinary a first-order L-S transition, the peak is rounded. Peak rounding is a common feature of ^{4}He in porous media [23]. Probably, the confinement of ^{4}He into the narrow pores and the pore-size distribution cause the broadening of the L-S transition.

In the inset of Fig. 2, we show the pressure dependence of the heat capacity at 0.8 K which is below the melting onset T_{MO}. The heat capacity suddenly decreases at

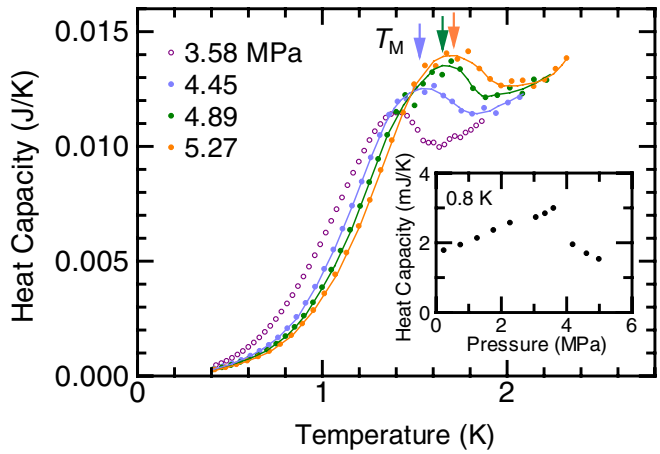

FIG. 2 (color online). Heat capacities of solid ^{4}He in the nanopores of Gelsil after the subtraction of the small contribution of bulk solid ^{4}He. The broad heat-capacity peak at a temperature denoted as T_M is caused by melting of ^{4}He in the nanopores. The solid lines are guides to the eye. Heat capacity of liquid ^{4}He at 3.58 MPa is also shown in the figure for comparison. Inset: Pressure dependence of the heat capacities at 0.8 K.

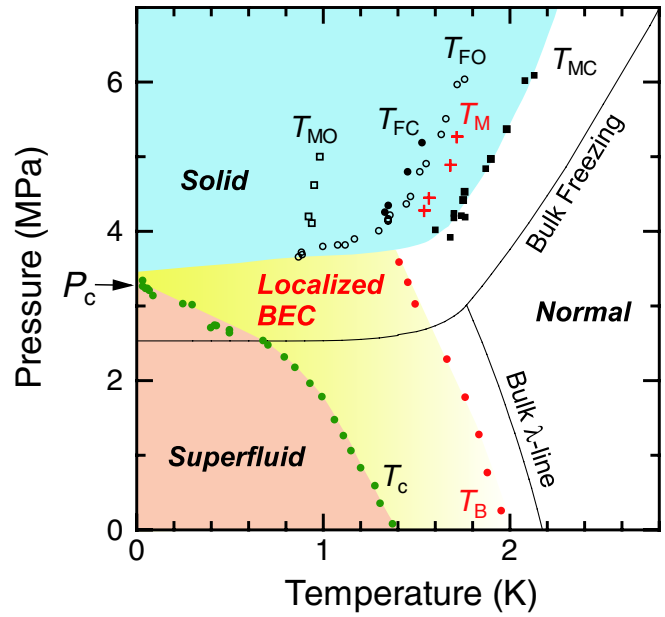

FIG. 3 (color online). The P-T phase diagram of ^{4}He in the 2.5-nm nanoporous glass determined in our present and previous studies [9,10]. The circles bordering the LBEC and normal phases and crosses indicate T_B and T_M in Figs. 1 and 2, respectively. T_c indicates the superfluid transition temperatures obtained in the TO study [9]. T_{FO} and T_{FC} indicate the freezing onset and the completion, and T_{MO} and T_{MC} indicate the melting onset and the completion, respectively [10]. P_c indicates a critical pressure, 3.4 MPa. The solid line shows the bulk λ line and the bulk L-S boundary.

$P \simeq 4$ MPa. This indicates that solid ^{4}He is formed in the nanopores and the contribution of the liquid decreases.

The heat-capacity peak temperatures T_B and T_M are plotted on the P-T phase diagram in Fig. 3. The T_B line is shifted from the bulk lambda line by 0.2 K and is located far above the superfluid T_c line. The peak temperature T_M is located between the freezing onset and melting completion lines obtained from the pressure studies [10].

The heat capacity of the liquid may have been interpreted as a finite-size effect of the superfluid transition in confined geometries [24]. However, T_B is much higher than the superfluid transition temperature T_c obtained in our TO study [9]. Therefore, the peak is not attributed to the superfluid transition but to some short-range order.

We assert that the heat-capacity peak indicates the formation of localized Bose-Einstein condensates (LBECs) on nanometer length scales. LBEC was first suggested in neutron scattering experiments for ^{4}He in Vycor and Gelsil at ambient pressure [11,12]. The LBEC originates from the spatial distribution of the Bose condensation temperature. Both the confinement and disorder produced by porous media may result in LBEC. Below T_B, many BECs start to form in favorable regions such as the largest pores, in which ^{4}He atoms can exchange their positions frequently. However, the exchange of atoms between BECs via unfavorable regions such as narrow pores is suppressed due to the hard core nature of ^{4}He. The suppression of atomic exchanges between the BECs results in the lack of global phase coherence in the whole system. Thus, the system does not exhibit superfluidity that is detected by macroscopic and dynamical measurements such as TO.

In neutron scattering experiments, roton signals that are unique to BEC have been observed above the superfluid T_c [11–13]. Moreover, in ^{4}He-filled Vycor, a broad heat-capacity peak was observed above T_c [21,25]. These results and our Gelsil result are mutually consistent and are most probably attributed to LBEC in the nanopores.

Theoretical studies have suggested that a random potential produced by a porous structure leads to the LBEC. Kobayashi and Tsubota studied strongly correlated ^{4}He in a 3D random environment. They found that superfluidity disappears above 4.2 MPa due to the localization of BEC [14]. A theory for a Bose gas with disorder at finite temperature suggests a locally condensed phase in which superfluidity does not occur [26]. Thus, these theories support the idea of LBEC.

The heat-capacity peak due to the formation of localized BECs resembles the peak by melting at higher pressures as shown in Fig. 2. This suggests that the change in the entropy associated with the LBEC-normal transformation is approximately equivalent to the entropy change in melting of a solid. We believe that this equivalence is reasonable, because the entropy of the LBEC state is comparable to that of the solid state [10].

No signature was observed in the heat capacity around T_c. In ^{4}He filled in Vycor, a very small peak was observed at T_c that is 0.02% of the size of the background heat capacity, in a high resolution measurement [21]. The resolution of our measurements is 1% and might be insufficient to resolve the small peak at T_c if the peak exists.

The existence of LBEC is further supported by heat capacity below T_B. Above 1 K, the heat capacity is explained well by roton excitations. The roton heat capacity is described by $C = AT^{-3/2}\exp(-\Delta/k_BT)$, where A is constant and Δ/k_B the roton energy gap. In Fig. 4(a), we plot $CT^{3/2}$ versus T^{-1}. The linear behavior proves the existence of rotons. The pressure dependence of Δ/k_B estimated from the fittings is shown in the inset of Fig. 4(a). As in the case of bulk ^{4}He [27], Δ/k_B decreases monotonically with pressure. Δ/k_B has a finite value 4.41 K at 3.60 MPa. It is important that the heat capacity above 2.5 MPa is well fitted to the roton term. Since T_c is well below 1 K in this pressure region, this observation proves that rotons, i.e., LBECs, exist in the nanopores well above T_c.

The roton contribution vanishes below 0.7 K. Instead, phonons are the significant excitations in this temperature region. In Fig. 4(b), we show the log-log plot of the heat capacities of liquid ^{4}He at $P < 3.58$ MPa with the data of the solid at 4.45 MPa. The heat capacities of the liquid are well fitted by T^3 below 0.7 K. This suggests that the heat capacity originates from 3D phonons. Below a temperature

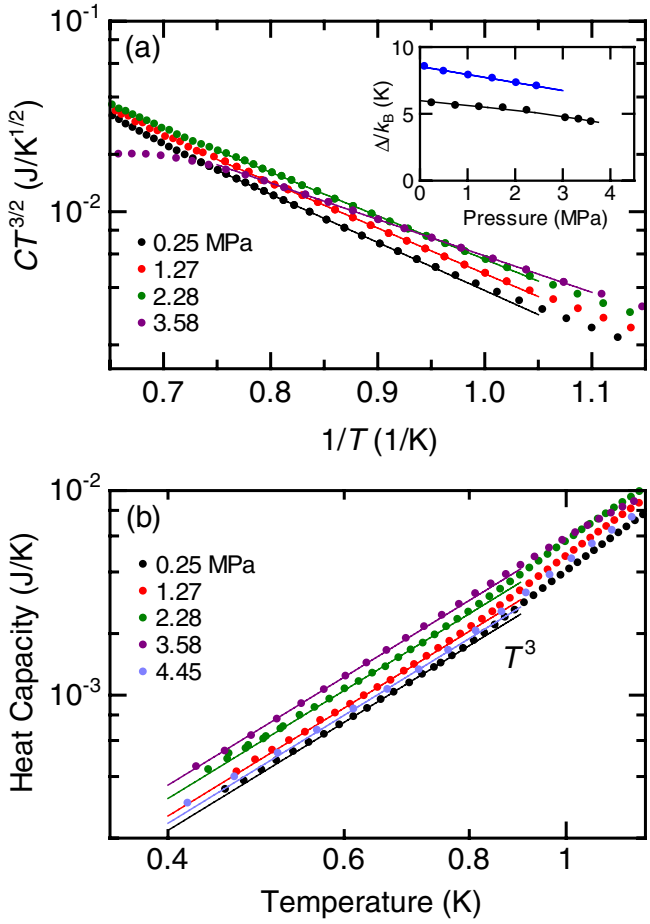

FIG. 4 (color online). (a) High-temperature heat capacities of liquid ^{4}He confined in Gelsil. The data are plotted as $CT^{3/2}$ vs T^{-1}. Inset: Pressure dependence of roton energy gap, Δ/k_B, of ^{4}He in Gelsil (lower line). The upper line shows Δ/k_B of bulk ^{4}He [27]. (b) Log-log plots of heat capacity at low temperatures. The solid lines are a fitting of T^3 to the data between 0.4–0.7 K.

$T_x \simeq hc/k_B\lambda_{\rm pore}$, where c is the sound velocity in a liquid and $\lambda_{\rm pore}$ the typical pore size, phonons with wavelengths greater than $\lambda_{\rm pore}$ are thermally excited and the 3D behavior is expected in the highly connected network of the nanopores [28]. If we use the sound velocity in bulk ^{4}He, $c = 2.39 \times 10^4$ cm/s, and $\lambda_{\rm pore} \sim 1.5$ nm assuming 1.5 inert layers [9], we obtain $T_x = 0.75$ K. This result is consistent with our observation. It is worth mentioning that our most recent measurements below 0.45 K show some deviation from the T^3 to T^2 behavior. This indicates that excitations other than phonons exist. Accurate measurements below 0.45 K will be essential to clarifying the nature of the low-energy thermal excitations at lower temperatures.

As well as in the liquid state, the heat capacity of the solid at 4.45 MPa is well fitted by T^3. This indicates that the heat capacity of the solid also originates from the 3D porous structure.

At 0 K, the P-T phase diagram implies that ^{4}He confined in the nanopores undergoes the superfluid-LBEC-solid QPT at P_c. The physics of this QPT is not clarified in our heat-capacity measurements because the lowest temperature of our measurements is 0.45 K. The heat-capacity study at lower temperatures near P_c is essential to reveal the entire nature of the QPT.

In conclusion, we have measured the heat capacity of ^{4}He confined in a 2.5-nm nanoporous glass. The heat capacity has a broad peak at temperature T_B that is much higher than T_c determined using the torsional oscillator technique. The heat capacities are well described by the excitations of phonons and rotons at all pressures. These observations strongly support the existence of nanoscale, localized Bose-Einstein condensates above T_c.

This work is supported by the Grant-in-Aid for Scientific Research on Priority Areas "Physics of Superclean Materials" from MEXT, Japan, and Grant-in-Aid for Scientific Research (A) from JSPS. K. Y. acknowledges the support of the JSPS.

[1] M. Greiner *et al.*, Nature (London) **415**, 39 (2002).
[2] L. Fallani *et al.*, Phys. Rev. Lett. **98**, 130404 (2007).
[3] L. Merchant *et al.*, Phys. Rev. B **63**, 134508 (2001).
[4] L. J. Geerligs *et al.*, Phys. Rev. Lett. **63**, 326 (1989).
[5] J. D. Reppy, J. Low Temp. Phys. **87**, 205 (1992).
[6] K. Shirahama *et al.*, Phys. Rev. Lett. **64**, 1541 (1990).
[7] N. Wada *et al.*, Phys. Rev. Lett. **86**, 4322 (2001).
[8] M. H. W. Chan *et al.*, Phys. Rev. Lett. **61**, 1950 (1988).
[9] K. Yamamoto *et al.*, Phys. Rev. Lett. **93**, 075302 (2004).
[10] K. Yamamoto *et al.*, J. Phys. Soc. Jpn. **77**, 013601 (2008).
[11] H. R. Glyde *et al.*, Phys. Rev. Lett. **84**, 2646 (2000).
[12] O. Plantevin *et al.*, Phys. Rev. B **65**, 224505 (2002).
[13] F. Albergamo *et al.*, Phys. Rev. B **76**, 064503 (2007).
[14] M. Kobayashi and M. Tsubota, arXiv:cond-mat/0510335; AIP Conf. Proc. **850**, 287 (2006).
[15] S. Miyamoto and Y. Takano, Czech. J. Phys. **46**, 137 (1996).
[16] T. Kobayashi *et al.*, AIP Conf. Proc. **850**, 277 (2006).
[17] K. Yamamoto *et al.*, J. Low Temp. Phys. **150**, 353 (2008).
[18] J. P. Shepherd, Rev. Sci. Instrum. **56**, 273 (1985).
[19] J. S. Brooks and R. J. Donnelly, J. Phys. Chem. Ref. Data **6**, 51 (1977).
[20] O. V. Lounasmaa, Cryogenics **1**, 212 (1961).
[21] G. M. Zassenhaus and J. D. Reppy, Phys. Rev. Lett. **83**, 4800 (1999); G. M. Zassenhaus and J. D. Reppy, J. Low Temp. Phys. **113**, 885 (1998); G. M. Zassenhaus, Ph.D. thesis, Cornell University, 1999.
[22] G. Ahlers, Phys. Rev. A **2**, 1505 (1970).
[23] D. F. Brewer *et al.*, Physica B (Amsterdam) **165&166**, 577 (1990).
[24] F. M. Gasparini and I. Rhee, in *Critical Behavior of Confined Helium*, edited by D. F. Brewer, Progress in Low Temperature Physics Vol. XIII (Elsevier, Amsterdam, 1992).
[25] D. F. Brewer, J. Low Temp. Phys. **3**, 205 (1970).
[26] A. V. Lopatin and V. M. Vinokur, Phys. Rev. Lett. **88**, 235503 (2002).
[27] O. W. Dietrich *et al.*, Phys. Rev. A **5**, 1377 (1972).
[28] K. G. Singh and D. S. Rokhsar, Phys. Rev. B **49**, 9013 (1994).